NASA Technical Memorandum 102288

Response of a Chemically Reacting Layer to Streamwise Vorticity

Russell W. Claus
Lewis Research Center
Cleveland, Ohio

December 1989

NASA Technical Memorandum 102288

Response of a Chemically Reacting Layer to Streamwise Vorticity

Russell W. Claus
Lewis Research Center
Cleveland, Ohio

National Aeronautics and
Space Administration

Lewis Research Center
Cleveland, Ohio 44135

Summary

A series of direct numerical simulations of a temporally evolving shear layer subject to both harmonic (two dimensional) and streamwise (three dimensional) forcing were performed. The interaction and coupling of these various two- and three-dimensional modes were shown to significantly alter the development of the flow. The scale of the three-dimensional modes was quite important to the coupling process, with greatly enhanced mixing and product formation resulting from three-dimensional modes that were rapidly amplified by the spanwise vorticity. In general, the longer wavelength three-dimensional modes were found to be highly efficient at increasing the momentum transport and the shorter wavelengths at increasing the mass transport.

Introduction

Controlling mixing in aeropropulsion devices is a key technology that can enable the development of advanced systems. In high-speed combustors the rapid mixing of reactants can lead to better control over local burning equivalence ratios, thereby reducing emissions of critical species such as oxides of nitrogen. In hypersonic applications whether or not the reactants mix is likely to determine the success of a particular scramjet reactor. In previous combustion devices mixing was controlled through the use of swirlers and multiport injection, but these devices can incur a significant pressure loss.

A great deal of interest has recently developed in the possible application of lobed mixers as a low-loss method for augmenting mixing in reacting flows (ref. 1). These lobed mixers increase mixing by promoting the development of streamwise vorticity. This streamwise vorticity generally takes the form of counterrotating vortex pairs that impart no net momentum to the flow field but can be quite effective in stirring (or mixing) the gas stream. Ideally an improved understanding of how to generate and amplify streamwise vorticity in a manner that encourages mixing could enable designers to better control combustion processes. But a series of questions arise such as, What scale should the streamwise vorticity be to get the strongest mixing? How do these structures affect the naturally occurring features of the flow? How can the maximum mixing be achieved with the lowest pressure drop?

A number of experiments have explored the role of streamwise vorticity in plane mixing layers (refs. 2 to 4). The recent study of reference 4 is of particular interest in relation to this report. In this experiment a corrugated splitter plate was used to generate a low-amplitude, three-dimensional perturbation that caused the development of streamwise vorticity. References 2 to 4 closely document several structural features of the shear layer that are referred to later in this report, but perhaps the most significant point is that the existence of a most unstable wavelength for the streamwise vorticity could not be identified. The three-dimensional instability was broadly amplified over a range between 1/5 and 3 times the Kelvin-Helmholtz wavelength. Reference 3 indicates that a wavelength approximately 0.67 of the spanwise wave (Kelvin-Helmholtz) is preferred, although again the authors felt that the amplification curve is broad. Some recent numerical calculations (ref. 5) have indicated that the growth of the three-dimensional instability is Reynolds number dependent, with the range of amplification being broadened at higher Reynolds numbers.

These streamwise vortices are difficult to quantitatively study experimentally. Despite the breadth of previous work, the study of how these structures affect both mass and momentum transport has not been fully resolved. Can a long-wavelength streamwise vortex pair lead to the rapid small-scale mixing that is needed for chemical reactions? Or is it more efficient to promote small-scale streamwise vortices that might not engulf as much of the reactants but would be faster at promoting mixing? The previous experiments and numerical studies do not resolve these questions. It was the purpose of the present study to explore these issues. A series of "numerical experiments" were designed to parametrically examine the effect of streamwise vorticity on a passive chemical reaction. A passive chemical reaction was used to avoid the further complicating effects of an exothermic chemical reaction on the flow field. In this study the flow field affected the chemical reaction, but the reaction did not affect the flow field.

Computational Approach

The term "direct numerical simulation" as used in this paper refers to the solution of the three-dimensional, time-dependent, Navier-Stokes equations by a highly accurate numerical scheme such that all the scales of motion are well resolved.

This definition imposes two major restrictions on the computational scheme. First, although highly accurate spectral methods are used to solve the governing equations, only a limited range of fluctuating motions can be resolved on the computational mesh. This limit restricts the calculations to a low-Reynolds-number flow (approximately 50 to 100 based on the Taylor microscale). When the results of a low-Reynolds-number calculation are applied to understanding high-Reynolds-number turbulence, an inherent assumption is that the large energetic scales of motion display characteristics that are Reynolds number independent. The second major limitation of these direct numerical simulations is that the use of spectral methods (Fourier series) imposed the need to use periodic boundary conditions in the main flow direction. Therefore these calculations are of a temporally evolving shear layer as opposed to spatially evolving laboratory experiments. This approach comprises a Lagrangian description of the spatially developing shear layer with the computation domain following the mean flow. The drawback that this approach imposed in comparisons with experimental data was offset by the greater numerical resolution available in the Lagrangian description of the flow. These temporally evolving simulations should be looked at as "idealizations" of the real flow.

The time-dependent Navier-Stokes equations were solved for incompressible flow with a single, scalar transport equation used to simulate a passive (no heat release), infinitely fast chemical reaction through a Shvab-Zeldovich transformation. This transformation provided the capability to examine the effect of mixing on a chemical reaction without the additional complications of variable density or finite rate chemistry. The system of differential equations was solved explicitly by using second-order accurate time differencing and pseudospectral approximations of the spatial field as noted in reference 6. Spherical wavenumber truncation was performed by following the method described in reference 7. The flow Reynolds number, based on the initial velocity thickness, was about 500.

The computational domain for these numerical simulations was sized to include one complete cycle of the forced (harmonic) wave in the X (axial) direction. The Y direction was typically more than three times this length, and the Z direction was equal to the X direction length. Grid points were equally spaced along each direction. (The orientation of these various axes is shown in figure 1.) Boundary conditions in the X and Z directions were periodic. In the Y direction no stress boundary conditions were used; quantities such as U (axial velocity) were set to provide a zero gradient across the boundary, and quantities such as V (radial velocity) were set to provide a reflection at the boundary.

The mean initial conditions for these simulations set the axial velocity to a hyperbolic tangent profile, similar to experimental values (ref. 8). Imposed on this mean field were perturbations that provided a harmonic (spanwise) vortex rollup and streamwise vorticity of various wavelengths that provided the rollup of the three-dimensional modes. The harmonic (spanwise) wave corresponded to the most unstable frequency as determined by linear stability theory. The three-dimensional modes developed from low-level perturbations (less than 2 percent of the mean). These perturbations started with a constant amplitude for all wavelengths.

The calculations were dimensioned such that the harmonic wavelength that led to the rollup of the spanwise vortex was equal to 2π. The longest three-dimensional mode studied was equal to this wavelength but was imposed in the cross-stream direction.

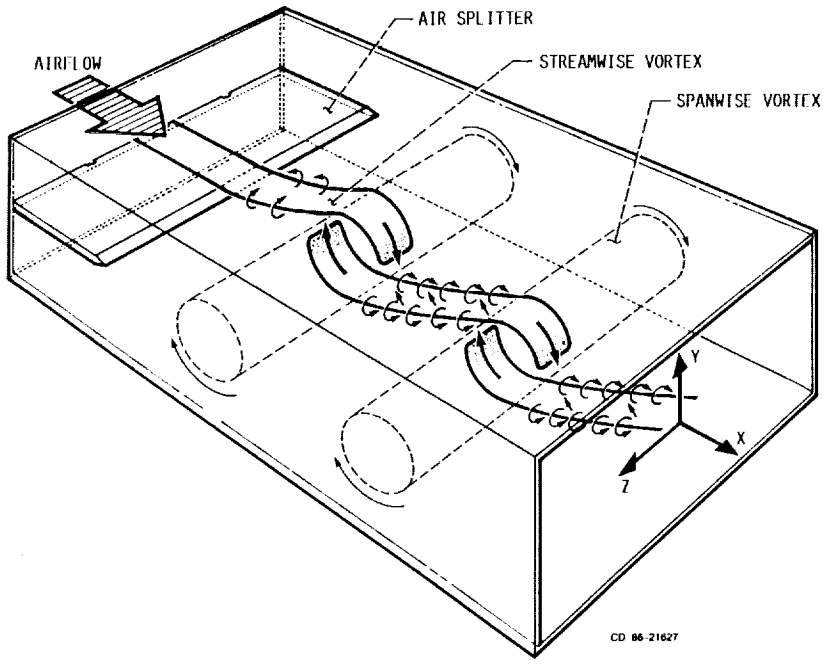

Figure 1.—Schematic representation of three-dimensional, plane shear layer.

The mean statistics determined from the calculations were integrations of the various quantities in the X and Z directions. This provided mean values as a function of the radial distance Y. The concentration thickness and the axial velocity thickness were established from these values. The integrated product was determined by integrating the product concentration in the X, Y, and Z directions.

Results and Discussion

Temporal Evolution of Typical Direct Numerical Simulation

The numerically simulated mixing layer is conceptually represented as shown in figure 1. The structure of typical streamwise and spanwise vorticity along with the orientation of the axes is illustrated.

The temporal evolution of a typical direct numerical simulation is illustrated in figures 2 to 4. In this simulation three-dimensional modes of a wavelength equal to $\pi/4$ interacted with the primary two-dimensional harmonic mode. Figure 2 displays how the mean axial velocity thickness, the concentration thickness, and the total integrated product developed as a function of time. (These temporal statistics can be related to spatial development in experiments through a Galiaen transformation (ref. 9) such that later times would correspond to farther distances downstream.) The velocity thickness is defined as the radial distance between the points where the mean axial velocity reaches 90 percent of $U_{+\infty}$ or $U_{-\infty}$ and is a measure of shear layer spreading. The concentration thickness is similarly defined as the radial distance between the points where the concentration thickness reaches 90 percent of $C_{+\infty}$ or $C_{-\infty}$. Initially, the spanwise vortex rolled up and saturated at approximately 10 seconds. After saturation the velocity thickness decreased, reaching a local minimum at approximately 20 seconds. There was then steady layer growth as the secondary instability increased. The concentration thickness initially grew faster than the velocity field. The concentration stopped spreading about the same time that the primary two-dimensional harmonic mode saturated. After about 24 seconds the secondary instability caused a steady increase in the mixing. The total amount of integrated product initially grew extremely slowly despite the early, rapid growth of the spanwise vortex. Somewhere around the time when the spanwise vortex saturated, the rate of product formation increased greatly. The rate of product formation diminished slightly at approximately 30 seconds but was still fairly high.

The momentum and mass transport rates are displayed in figure 3 for representative times in the simulation. The Reynolds stresses (momentum transport) were initially negative (at 6 sec), indicating gradient transport and a rapid growth of the shear layer. At 12 seconds the Reynolds stresses changed sign and indicated countergradient transport, where energy is transferred from the turbulence to the mean flow.

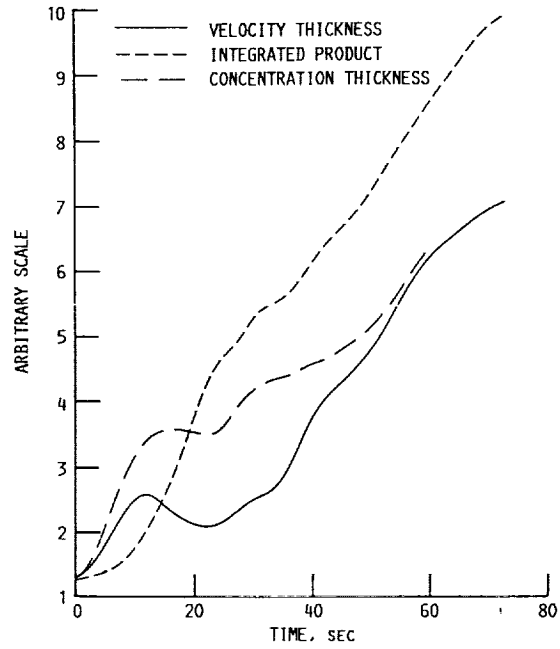

Figure 2.—Development of total integrated product, concentration thickness, and axial velocity thickness for direct numerical simulation with streamwise forcing at wavelength of $\pi/2$.

The shear layer velocity thickness decreased correspondingly as shown in figure 2. The Reynolds stresses changed sign again at 24 seconds and became more negative at later times. The Reynolds stresses indicated countergradient transport for times between 12 and 18 seconds. The mass transport stress $\overline{vf}$ indicated a much shorter period of countergradient transport and as a result did not greatly retard the rate of mixing. It is interesting that there was such a marked disparity between momentum and mass transport. Apparently, the scale of the streamwise vorticity can affect mass and momentum transport in different ways as is more clearly illustrated in later figures.

It has been well established experimentally (ref. 4) that the two-dimensional harmonic (spanwise) wave initially rolls up and saturates before the secondary three-dimensional instability forms. This can be observed in figure 4. In figures 4(a) to (d) the product field is displayed in two different cross sections. A cross section was made in the Z–Y plane that cut through the braid region of the spanwise vortex. The secondary instability was visible in this cross section. A second cross section made in the X–Y plane displayed the rollup of the spanwise vortex. In both of these planes the highest level of product is displayed as yellow. At early times (fig. 4(a)) the product field clearly displayed the rollup of the spanwise vortex in the X–Y plane. In the Z–Y plane the streamwise vorticity only slightly distorted the interface. At later times, from 36 seconds on, the spanwise vorticity strongly stretched the streamwise vorticity, and the main increase in product appeared to be due to the increased mixing in the Z–Y plane. In fact at 45 seconds the size of the spanwise vortex appeared to be diminished and the braid region exhibited high levels of product. By 54 seconds the mushroom-shaped structures

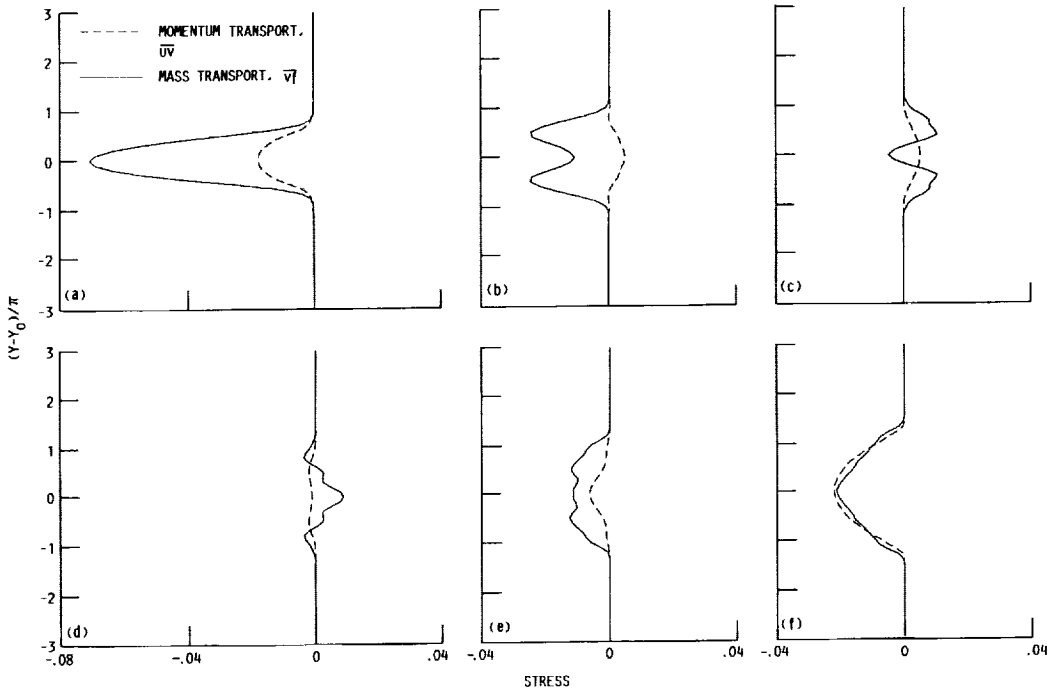

(a) Time, 6 sec. (b) Time, 12 sec. (c) Time, 18 sec.
(d) Time, 24 sec. (e) Time, 30 sec. (f) Time, 45 sec.

Figure 3.—Mass and momentum transport rates at representative times for direct numerical simulation with streamwise forcing at wavelength of $\pi/2$.

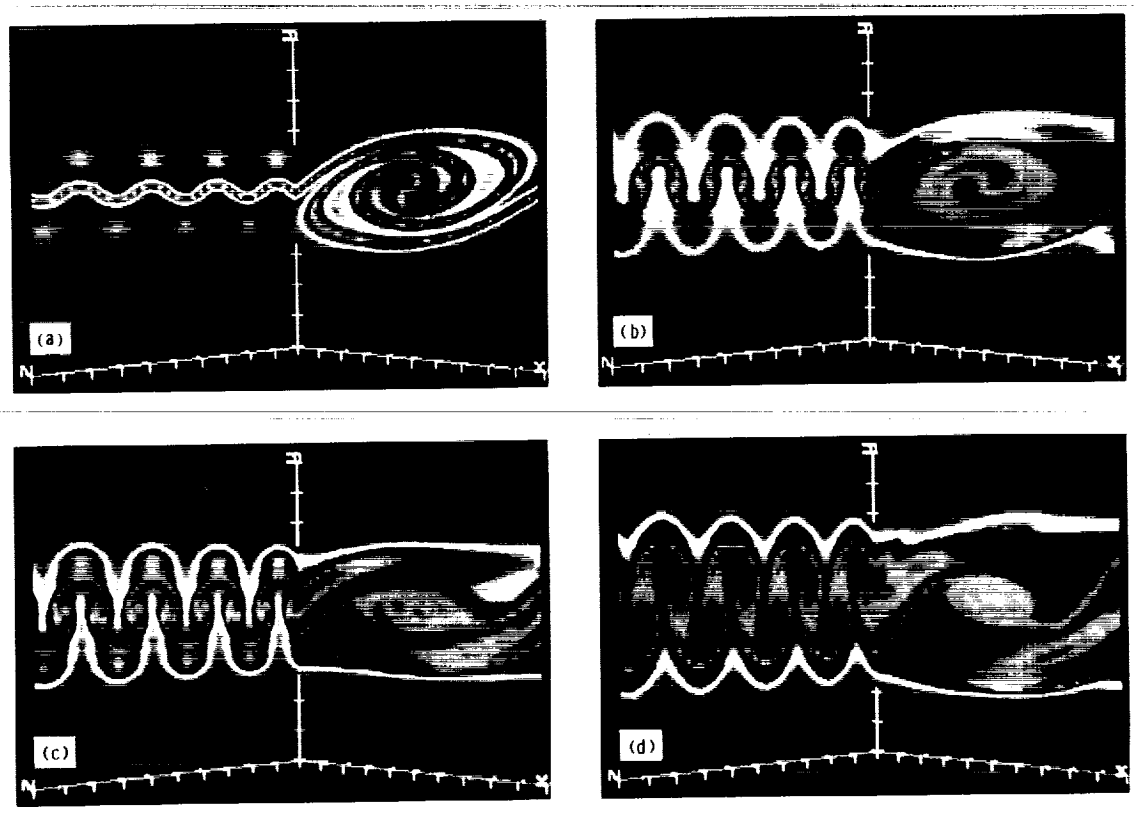

(a) Time, 18 sec. (b) Time, 36 sec.
(c) Time, 45 sec. (d) Time, 54 sec.

Figure 4.—Product field cross sections at representative times in Z-Y plane through braids and in X-Y plane through spanwise vortex. Yellow indicates the highest concentration of product. Streamwise forcing is at a wavelength of $\pi/2$.

formed by the counterrotating streamwise vortices appeared to dominate the spanwise vortex.

It is instructive to more closely examine the structure of these counterrotating vortex pairs and how they affect the vortex and the product field. Figure 5 displays Z–Y cross sections for a "numerical experiment" where the streamwise vorticity was forced at a wavelength of 2π. These results are all for a time of 60 seconds. This cross-sectional view was selected to cut through the core of the spanwise vortex in a manner that would illustrate the secondary instability. The product field is displayed in figure 5(a). Quite clearly visible in this cross section is the high level of product formed by the spanwise vortex. The two "bumps", both above and below the spanwise vortex core, formed because of the counterrotating vortex pairs. The formation of these "bumps" at staggered locations on opposite sides of the spanwise vortex was not due to the initial conditions of the calculation. Initially only one counterrotating pair was introduced into the calculations and staggering occurred naturally in the simulation. This staggering is in strong agreement with the experimental findings of reference 4, where a similar phenomenon was observed.

The streamwise vorticity through the core of the spanwise vortex is displayed in figure 5(b). Several counterrotating vortex pairs are evident in the calculation. In or near the core of the spanwise vortex an image pair of counterrotating vortices formed. These vortices were quite strong, and they

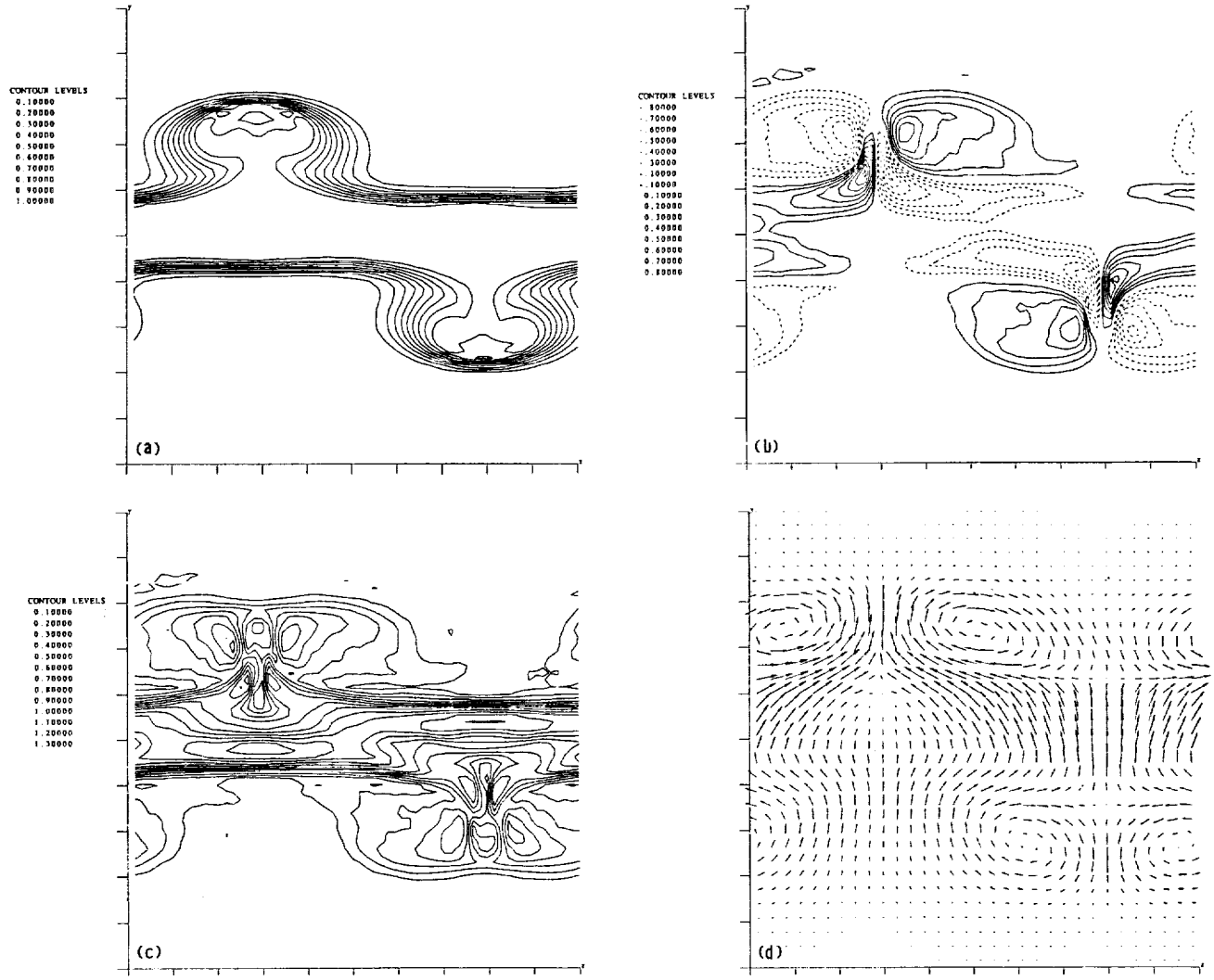

(a) Product field through spanwise vortex core.
(b) Streamwise vorticity through spanwise core.
(c) Total vorticity through spanwise vortex core.
(d) Secondary velocities through spanwise core.

Figure 5.—Various quantities in Z–Y plane through spanwise vortex core displaying structure of counterrotating streamwise vortices. Results are from a numerical simulation with streamwise forcing at a wavelength of 2π.

may have helped to improve circulation and mixing in the spanwise vortex. The total vorticity field (fig. 5(c)) shows that these structures were dynamically significant.

The secondary velocity field (V and W) is shown in figure 5(d). Here the dominant circulation pattern was due to the counterrotating vortex pairs. The image vortices augmented this circulation pattern. Somewhat surprisingly, some of the highest secondary velocities were induced in the spanwise vortex.

Effect of Streamwise Vorticity Scale

A series of numerical simulations were performed to explore the effect of streamwise vorticity scale on the rate of product formation. These simulations were conducted as "numerical experiments," where every parameter in the calculation was kept constant except the wavelength of the streamwise vorticity imposed as an initial condition. The scale of the streamwise perturbations used in the experiments was selected to bracket the wavelength experimentally estimated to be the most amplified mode (ref. 3).

The amount of product formed in a series of these numerical experiments is displayed in figure 6. The solid line provides a baseline case in which no streamwise vorticity was included in the initial conditions and the amount of product formed was due only to the spanwise vortex rollup. This case is also equal to the case of streamwise forcing at a wavelength of $\pi/4$.

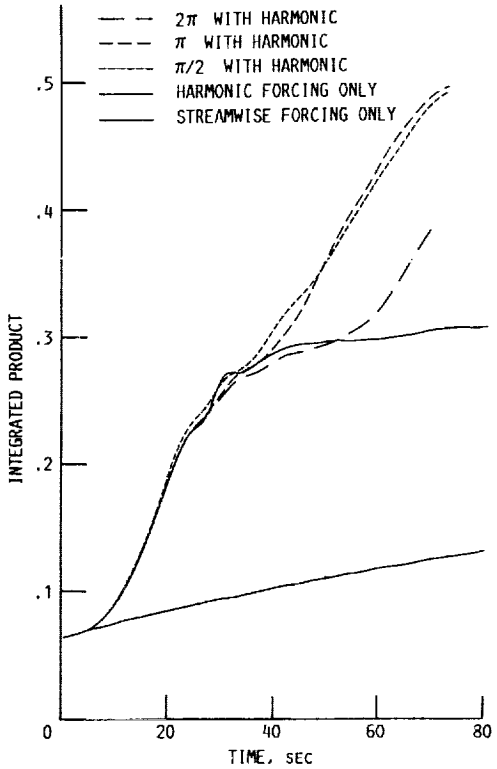

Figure 6.—Temporal development of total integrated product for series of numerical simulations with streamwise forcing at various wavelengths.

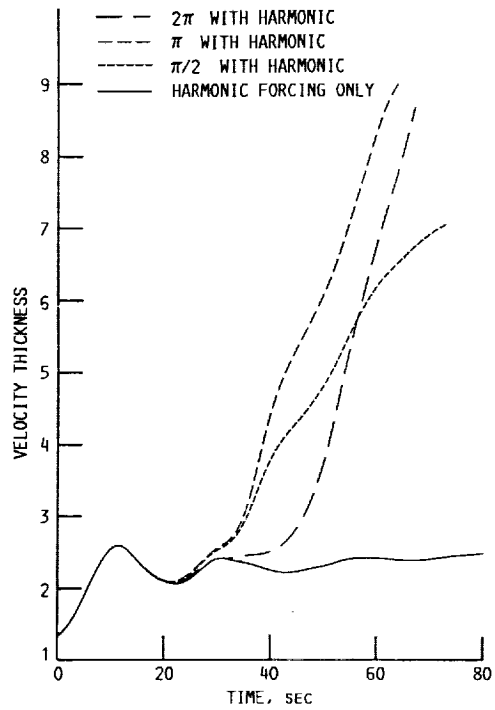

Figure 7.—Temporal development of axial velocity thickness for numerical simulations with streamwise forcing at various wavelengths.

Apparently an extremely short wavelength such as $\pi/4$ is not significantly amplified by the spanwise vortex. As a result the amount of product formed was dominated by the rollup of the spanwise vortex. For longer wavelengths, however, the results were much different although the early development of all of the simulations with streamwise forcing was initially dominated by the rollup of the spanwise vortex. After about 30 seconds the streamwise vorticity was sufficiently amplified to have a marked effect on the total amount of product formed. Streamwise forcing in a wavelength range of π to $\pi/2$ resulted in very similar high levels of product formation. Forcing at a wavelength of 2π required more time for the effect to be discernible. Whereas wavelengths of π or $\pi/2$ displayed increased levels of product from approximately 30 seconds, forcing at 2π did not indicate a significant increase until about 55 seconds.

Also displayed in figure 6 is the result of a simulation with only streamwise forcing. In this case there was no rollup of the spanwise vortex—correspondingly much less product was formed. This result indicates that streamwise vorticity has a highly nonlinear effect on product formation.

The effect of streamwise vorticity on shear layer growth is displayed in figure 7. As in the previous figure, a calculation with only two-dimensional harmonic forcing is shown as a baseline. For the mean axial velocity the most amplified mode had a wavelength of π. The $\pi/2$ results provided significantly less spreading for times greater than 40 seconds. An interesting difference is seen in the 2π results. Although forcing at this wavelength was slower to indicate any difference from the

purely two-dimensional calculation, when the effect of forcing became noticeable, the growth rate was almost explosive. For times greater than about 55 seconds the 2π forcing calculation displayed a higher level of spreading than the $\pi/2$ calculation.

The concentration thickness, which is a direct measure of mixing, is displayed in figure 8. This parameter displayed the same type of behavior as the axial velocity thickness. In the region where the secondary instability was significant in increasing mixing, the long wave, 2π, showed a delayed effect but eventually reached the same strong level of mixing as the shorter π wavelength. The short wavelength, $\pi/2$, generally was least efficient in promoting mixing.

In several ways the results of the axial velocity field were different from the results of the total integrated product. First, although forcing at π and $\pi/2$ produced roughly the same amount of product, the longer wavelength was much more effective in increasing the momentum transport. Second, the longest wavelength, 2π, required more time to be significantly amplified, but when the three-dimensional waves were amplified, they were extremely efficient at increasing the momentum transport.

If the axial velocity spread was dissimilar from the product field, was there a parameter that seemed to correlate well? Figure 9 displays the maximum absolute vorticity in the X direction ω_x for the various numerical experiments. In this figure the streamwise vorticity exhibits an almost exponential

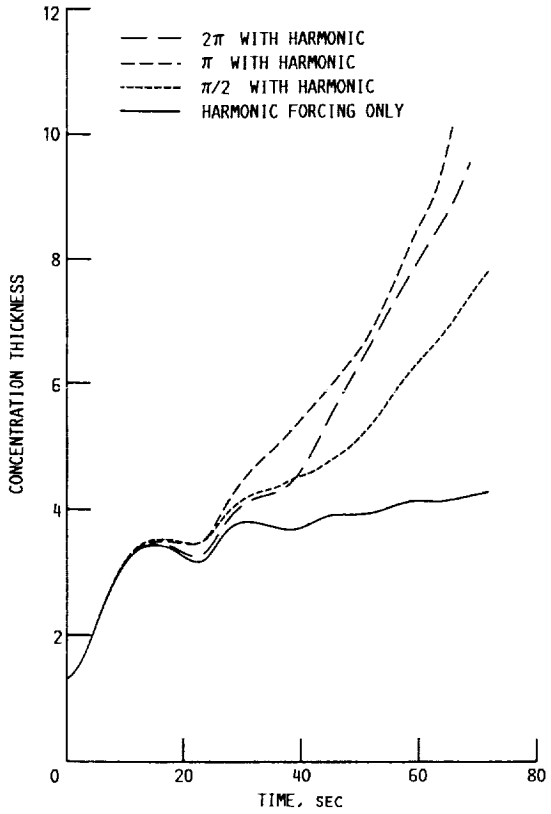

Figure 8.—Temporal development of concentration thickness for numerical simulations with streamwise forcing at various wavelengths.

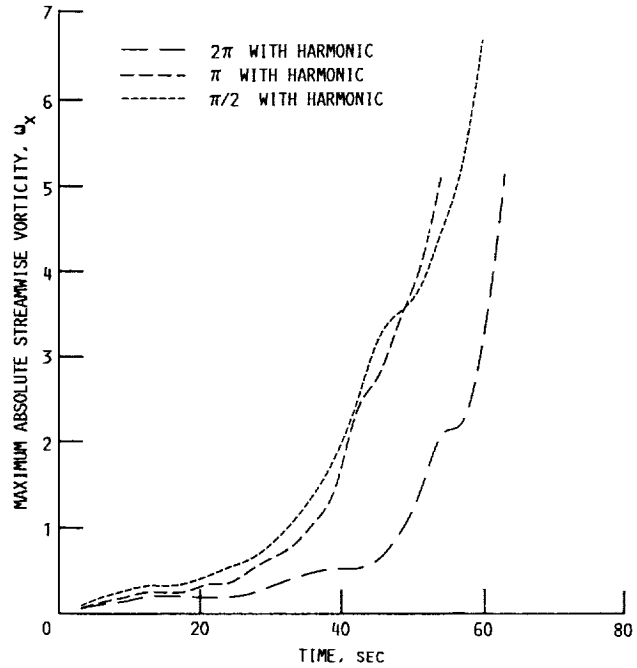

Figure 9.—Temporal development of maximum absolute streamwise vorticity for numerical simulations with streamwise forcing at various wavelengths.

growth for times greater than 30 seconds. Streamwise forcing at π and $\pi/2$ appeared to be fairly equally amplified. Forcing at 2π took much longer to increase, but after about 50 seconds the growth of the streamwise vorticity was quite strong. These results correlated well with the product formation shown in figure 6.

Certain structural aspects of the vorticity shear layer may explain how the amplification of the streamwise vorticity occurred. Figure 10 displays the total and streamwise vorticity for two cases of forcing at $\pi/2$ and 2π. The short-wavelength forcing resulted in streamwise structures that were perpendicularly alined with the spanwise vortex. This resulted in the streamwise rollers being alined along the axis of greatest shear in the braid region. For the longer wavelength simulation, however, the streamwise vortices were not initially alined along the greatest shear axis, and this probably explains the delay in amplification seen in figure 9. The slight angle of the long-wavelength streamwise vorticity appeared to be more efficient at removing energy from the spanwise vortex. The total vorticity in figure 10(d) was completely dominated by the streamwise structures; in figure 10(b) the spanwise vortex was still significant although it was clearly dominated by the streamwise vortex.

Concluding Remarks

The question of how these findings would change at higher Reynolds numbers was not addressed in this study and remains a logical extension of this work. Reference 5 has indicated

ORIGINAL PAGE
COLOR PHOTOGRAPH

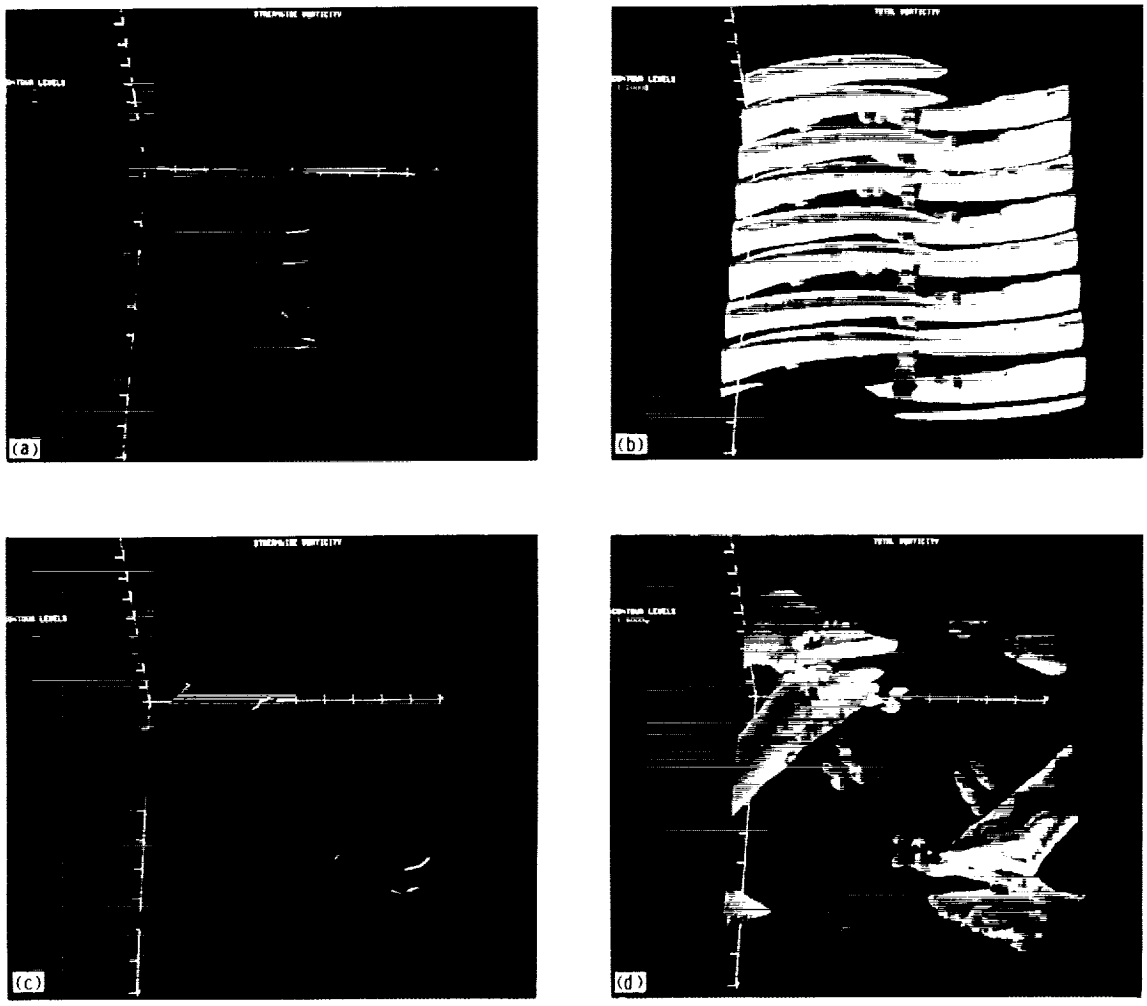

(a) Streamwise vorticity for $\pi/2$ forcing. Cyan denotes positive vorticity; magenta, negative vorticity.
(b) Total vorticity for $\pi/2$ forcing.
(c) Streamwise vorticity for 2π forcing. Cyan denotes positive vorticity; magenta, negative vorticity.
(d) Total vorticity for 2π forcing.

Figure 10.—Total and streamwise vorticity in two different numerical simulations.

that the longer wavelengths may be more rapidly amplified at higher Reynolds numbers. It seems logical that this would increase product formation and thereby provide a range of scales that are effective at increasing both mass and momentum transport.

Summary of Results

This paper explored whether it is more effective to augment mixing and chemical reaction through short or long wavelength streamwise forcing. The scale of the streamwise forcing was shown to have different effects on three parameters; product formation, momentum transport, and mass transport. To maximize product formation, forcing in a range approximately one-half to one-fourth of the spanwise wavelength was the preferred range. (In this paper the spanwise wavelength was defined as 2π.) However, if it is desired to augment the momentum transport, then longer wavelengths such as one to one-half of the spanwise wavelength were perferred. To achieve both increased momentum and mass transport, forcing at one-half the spanwise wavelength appeared to be ideal.

References

1. McVey, J.B.; and Kennedy, J.B.: Flame Propagation Enhancement Through Streamwise Vorticity Stirring. AIAA Paper 89-0619, Jan. 1989.
2. Konrad, J.H.: An Experimental Investigation of Mixing in Two-Dimensional Turbulent Shear Flows With Applications to Diffusion-Limited Chemical Reactions. PhD. Thesis, California Institute of Technology, 1976.
3. Bernal, L.P.; and Roshko, A.: Streamwise Vortex Structure in Plane Mixing Layers. J. Fluid Mech., vol. 170, Sept. 1986, pp. 499-525.
4. Lasheras, J.C.; and Choi, H.: Three-Dimensional Instability of a Plane Free Shear Layer: An Experimental Study of the Formation and Evolution of Streamwise Vortices. J. Fluid Mech., vol. 189, Apr. 1988, pp. 53-86.
5. Metcalfe, R.W., et al.: Secondary Instability of a Temporally Growing Mixing Layer. J. Fluid Mech., vol. 184, Nov. 1987, pp. 207-243.
6. McMurthry, P.A., et al.: Direct Numerical Simulations of a Reacting Mixing Layer With Chemical Heat Release. AIAA J., vol. 24, no. 6, June 1986, pp. 962-970.
7. Patterson, G.S., Jr.; and Orszag, S.A.: Spectral Calculations of Isotropic Turbulence: Efficient Removal of Aliasing Interactions. Phys. Fluids, vol. 14, no. 11, Nov. 1971, pp. 2538-2541.
8. Michalke, A.: On the Inviscid Instability of the Hyperbolic-Tangent Velocity Profile. J. Fluid Mech., vol. 19, Aug. 1964, pp. 543-556.
9. Orszag, S.A.; and Pao, Y.H.: Numerical Computation of Turbulent Shear Flows. Turbulent Diffusion in Environmental Pollution, Advances in Geophysics, Vol. 18A, F.N. Frenkiel and R.E. Munn, eds., Academic Press, 1974, pp. 225-236.

NASA
National Aeronautics and Space Administration

Report Documentation Page

1. Report No.	2. Government Accession No.	3. Recipient's Catalog No.
NASA TM-102288		

4. Title and Subtitle	5. Report Date
Response of a Chemically Reacting Layer to Streamwise Vorticity	December 1989
	6. Performing Organization Code

7. Author(s)	8. Performing Organization Report No.
Russell W. Claus	E-4956
	10. Work Unit No.
	505-62-21

9. Performing Organization Name and Address	11. Contract or Grant No.
National Aeronautics and Space Administration Lewis Research Center Cleveland, Ohio 44135-3191	
	13. Type of Report and Period Covered
	Technical Memorandum

12. Sponsoring Agency Name and Address	14. Sponsoring Agency Code
National Aeronautics and Space Administration Washington, D.C. 20546-0001	

15. Supplementary Notes

16. Abstract

A series of direct numerical simulations of a temporally evolving shear layer subject to both harmonic (two dimensional) and streamwise (three dimensional) forcing were performed. The interaction and coupling of these various two- and three-dimensional modes were shown to significantly alter the development of the flow. The scale of the three-dimensional modes was quite important to the coupling process, with greatly enhanced mixing and product formation resulting from three-dimensional modes that were rapidly amplified by the spanwise vorticity. In general, the longer wavelength three-dimensional modes were found to be highly efficient at increasing the momentum transport and the shorter wavelengths at increasing the mass transport.

17. Key Words (Suggested by Author(s))	18. Distribution Statement
Turbulence control Direct numerical simulation	Unclassified – Unlimited Subject Category 34

19. Security Classif. (of this report)	20. Security Classif. (of this page)	21. No of pages	22. Price*
Unclassified	Unclassified	10	A03

*For sale by the National Technical Information Service, Springfield, Virginia 22161